Fitoterapia 100 (2015) 68–74

Contents lists available at ScienceDirect

Fitoterapia

journal homepage: www.elsevier.com/locate/fitote

# Natural phosphodiesterase-4 inhibitors from the leaf skin of *Aloe barbadensis* Miller

Jia-Sheng Zhong [a], Yi-You Huang [a], Tian-Hua Zhang [a], Yu-Peng Liu [a], Wen-Jing Ding [a], Xiao-Fang Wu [b,c], Zhi-Yong Xie [a], Hai-Bin Luo [a,*], Jin-Zhi Wan [a,*]

[a] School of Pharmaceutical Sciences, Sun Yat-sen University, Guangzhou 510006, PR China
[b] Analysis and Testing Center, Chinese Academy of Tropical Agricultural Sciences, Haikou 571101, PR China
[c] Hainan Provincial Key Laboratory of Quality and Safety for Tropical Fruits and Vegetables, Haikou 571101, PR China

ARTICLE INFO

*Article history:*
Received 14 October 2014
Accepted in revised form 19 November 2014
Available online 28 November 2014

*Chemical compounds studied in this article:*
Isoaloeresin D (PubChem CID: 76332505)
Aloin B (PubChem CID: 5458894)
Aloin A (PubChem CID: 5458893)
Aloe-emodin (PubChem CID: 10207)
Aloinoside B (PubChem CID: 46173998)
Aloinoside A (PubChem CID: 46173997)

*Keywords:*
*Aloe barbadensis* Miller
Anthrone
Chromone
PDE4
Cytotoxicity

ABSTRACT

The ethanolic extract of *Aloe barbadensis* Miller leaf skin showed inhibitory activity against phosphodiesterase-4D (PDE4D), which is a therapeutic target of inflammatory disease. Subsequent bioassay-guided fractionation led to the isolation of two new anthrones, 6′-*O*-acetyl-aloin B (**9**) and 6′-*O*-acetyl-aloin A (**11**), one new chromone, aloeresin K (**8**), together with thirteen known compounds. Their chemical structures were elucidated by spectroscopic methods including UV, IR, 1D and 2D NMR, and HRMS. All of the isolates were screened for their inhibitory activity against PDE4D using tritium-labeled adenosine 3′,5′-cyclic monophosphate ($^3$H-cAMP) as substrate. Compounds **13** and **14** were identified as PDE4D inhibitors, with their $IC_{50}$ values of 9.25 and 4.42 μM, respectively. These achievements can provide evidences for the use of *A. barbadensis* leaf skin as functional feed additives for anti-inflammatory purpose.



## 1. Introduction

*Aloe barbadensis* Miller, also known as “true aloe”, is a medicinal and edible plant widely distributed in Europe, Asia and southern parts of North America [1,2]. In general, its leaf can be divided into three major parts, the outer green leaf skin, the inner clear pulp and the bitter yellow exudate secreted by vascular bundles [3]. The pulp (aloe gel) is widely used for cosmetics, beverage and nutraceutical [4], and the exudate composed of phenolic compounds [5] has a long history of medical use such as being a laxative [6], anti-oxidant [7] and anti-cancer agents [8]. Instead, it seems that the leaf skin part of *A. barbadensis* is regarded as solid waste generated during the processing. Excitingly, recent studies and our preliminary experiments have demonstrated that *A. barbadensis* leaf skin extract could serve as functional feed additives for immunity enhancement and anti-inflammatory purposes [9], which makes it possible to turn trash into treasure. However, the compositions of *A. barbadensis* leaf skin have rarely been reported. For further studies, it is urgent to clarify its chemical constituents and corresponding bioactivity.

The phosphodiesterases (PDEs) are a superfamily of enzymes that catalyze the hydrolysis of the intracellular second messengers cyclic adenosine monophosphate (cAMP) and cyclic guanosine monophosphate (cGMP) [10]. Among the eleven PDE families categorized by the human genome encoding, the cAMP-specific PDE4, which is mainly distributed

* Corresponding authors. Tel.: +86 20 39943031; fax: +86 20 39943040.
*E-mail addresses:* luohb77@mail.sysu.edu.cn (H.-B. Luo), jinzhiwan2004@aliyun.com (J.-Z. Wan).

http://dx.doi.org/10.1016/j.fitote.2014.11.018
0367-326X/

in immune and inflammatory cells, has gained increasing attention [11]. PDE4 is involved in inflammatory responses and is proven as targets for the treatments of chronic obstructive pulmonary disease (COPD), asthma and central nervous system (CNS) disease [12–14]. Recent research also demonstrated that PDE4 is bound up with anti-aging, reducing stroke risk, and treating memory loss associated with Alzheimer's disease [15–17], which make it a research hotspot.

Our previous report indicated that *A. barbadensis* extract and several compounds possessed anti-inflammatory properties through inhibiting the activity of PDE4D [18]. In continuation, it was found that the ethanolic extract of *A. barbadensis* leaf skin showed similar effects as well. Subsequent phytochemical investigation led to the isolation of two new anthrones (**9** and **11**), one new chromone (**8**), together with thirteen known compounds (Fig. 1). All of the isolates were screened for their inhibitory activity against PDE4D. As a result, compounds **13** and **14** were identified as PDE4 inhibitors, with their $IC_{50}$ values less than 10 μM. Herein, the details of the isolation, structural elucidation and the PDE4 inhibitory activity assay of these compounds are described.

## 2. Experimental

### 2.1. General

Optical rotations were measured on a Rudolph Autopol I automatic polarimeter (Rudolph Research Analytical, Hackettstown, NJ, USA) with MeOH as solvent. UV spectra were recorded on a Shimadzu UV2457 spectrophotometer (Kyoto, Japan) and IR spectra were obtained with a Bruker Tensor 37 FT-IR spectrophotometer (Bruker Optics Inc., Billerica, MA, USA) with KBr pellets. NMR spectra were acquired using a Bruker AVANCE 400 spectrometer (Bruker Biospin GmbH, Rheinstetten, Germany) and chemical shifts ($\delta$) were given in ppm with TMS as internal standard. ESIMS data were determined on a TSQ Quantum mass spectrometer (Thermo Finnigan LLC, San Jose, CA, USA) and high-resolution mass spectra (HRMS) were obtained on a Shimadzu LCMS-IT-TOF hybrid mass spectrometer (Kyoto, Japan). Semi-preparative RP-HPLC was performed on a Shimadzu LC-20AT liquid chromatography system (Kyoto, Japan) equipped with two LC-20AT pumps and a dual wavelength UV-VIS detector monitoring at 300 and 355 nm. A semi-preparative ODS-A column (250 × 10 mm i.d., 5 μm, YMC Co., Ltd., Kyoto, Japan) was employed for the separation at a flow rate of 3.0 mL $min^{-1}$. Reversed-phase flash chromatography (RP-FC) was achieved on a Biotage Isolera flash purification system (Biotage AB, Uppsala, Sweden) coupled with an Eyela glass column (300 × 20 mm i.d., Tokyo, Japan) packed with RP-$C_{18}$ gel (20–40 μm, Fuji Silisia Chemical Ltd., Nagoya, Japan). Silica gel (300–400 mesh) used for column chromatography was produced by Qingdao Marine Chemical Co., Ltd. (Qingdao, China). Thin layer chromatography (TLC) was carried out on silica gel G precoated plates (Qingdao Marine Chemical Co., Ltd., Qingdao, China) and spots were visualized under UV 254 and/or 365 nm or by spraying with

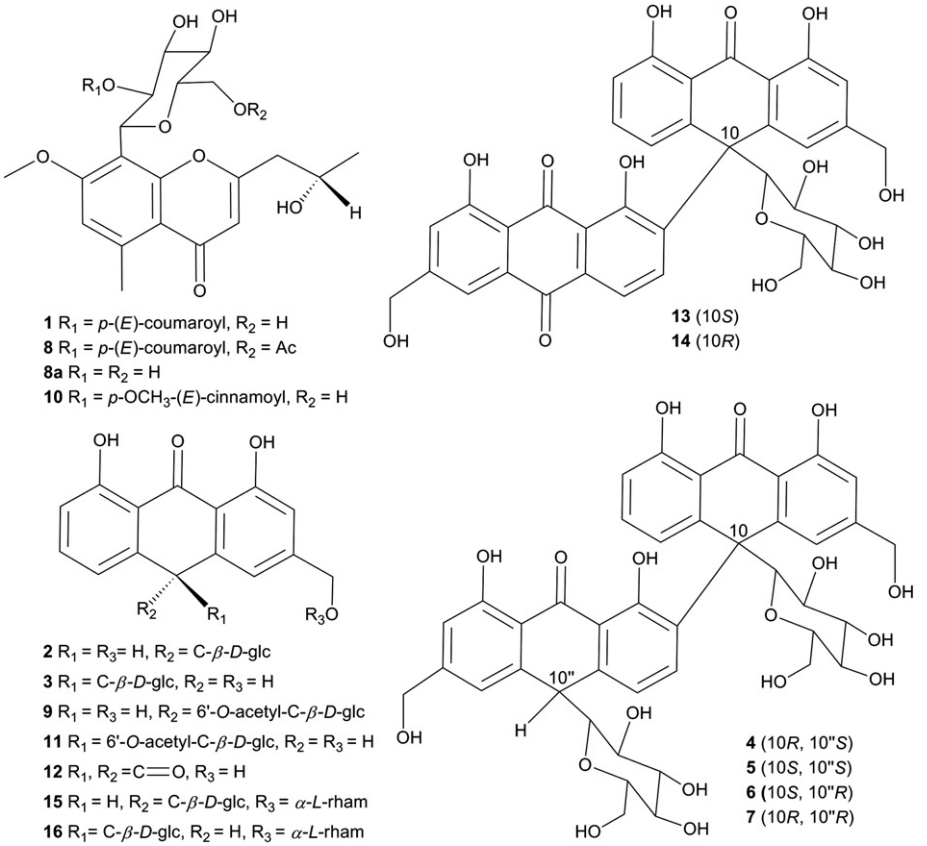


**Fig. 1.** Chemical structures of compounds **1**–**16**.

10% $H_2SO_4$ in EtOH (v/v) followed by heating. Methanol used for HPLC analysis was of HPLC grade and purchased from SK Chemicals (Ulsan, Korea). Ultrapure water was obtained from a Milli-Q laboratory water purification system (Millipore, Bedford, MA, USA). Other solvents were of analytical grade and manufactured by Tianjin Zhiyuan Chemical Reagent Co., Ltd. (Tianjin, China). UP200S ultrasonic cell disruption processor (Hielscher, Teltow, Germany), 6K15 centrifugal machine (Sigma, Santa Clara, CA, USA), BioPhotomer spectrophotometer (Eppendorf, Hamburg, Germany) and nickel-nitriloacetic acid (Ni-NTA) column (Qiagen, Hilden, Germany) were employed for the expression and purification of PDE4D. The radioactivity of the samples was measured on a Tricarb 2910 liquid scintillation counter (PerkinElmer, Waltham, MA, USA). LB medium was prepared using yeast extract and tryptone purchased from Oxoid Ltd. (Basingstoke, England). The isotope labeled substrate $^3$H-cAMP was manufactured by GE Healthcare (Waukesha, WI, USA). 3-(4,5-Dimethylthiazol-2-yl)-2,5-diphenyltetrazolium bromide (MTT) was obtained from Amresco Inc. (Solon, OH, USA). Other reagents such as positive control rolipram were purchased from Sigma (Santa Clara, CA, USA).

### 2.2. Plant material

The *A. barbadensis* leaf skin powder was provided by Yunnan Evergreen Biological Co., Ltd. (Yuxi, China) and was originally collected from Yunnan Province, China. The plant was authenticated by one of the authors, Prof. Jin-Zhi Wan. A voucher specimen (No. 20131202) was deposited at School of Pharmaceutical Sciences, Sun Yat-sen University, Guangzhou, China.

### 2.3. Extraction and isolation

The dried and powdered leaf skin of *A. barbadensis* (500.0 g) was extracted three times with 95% EtOH (3 × 1 L) under ultrasonic. The extract was filtered and concentrated under reduced pressure to yield a dark residue (34.3 g). The crude ethanolic extract was suspended in distilled water (500 mL) and fractionated successively with 3 × 500 mL volumes of petroleum ether, EtOAc and *n*-butanol. The EtOAc fraction (8.1 g) was then subjected to RP-FC and eluted with a gradient of MeOH–$H_2O$ (30:70 to 80:20, v/v) at a flow rate of 20 mL min$^{-1}$ to afford 10 fractions (E1–E10). Fraction E3 was further chromatographed by RP-FC using MeOH–$H_2O$ (26:74, v/v) as mobile phase to yield compounds **1** (321 mg), **2** (362 mg) and **3** (738 mg). Fraction E5 was purified by semi-preparative HPLC using a MeOH–$H_2O$ (56:44, v/v) system to obtain compounds **4** (3 mg, $t_R$ 11.5 min), **5** (2 mg, $t_R$ 12.3 min), **6** (3 mg, $t_R$ 13.2 min) and **7** (4 mg, $t_R$ 13.9 min). Fraction E6 was subjected to semi-preparative HPLC eluted with an isocratic elution system of MeOH–$H_2O$ (60:40, v/v) to give compounds **8** (45 mg, $t_R$ 8.9 min) and **9** (63 mg, $t_R$ 13.5 min). Using the same procedure, compounds **10** (23 mg, $t_R$ 13.4 min) and **11** (82 mg, $t_R$ 15.7 min) were obtained from fraction E7. Fraction E9 was chromatographed on silica gel column (100 × 10 mm i.d.) eluted with a step gradient of $CH_2Cl_2$–MeOH (10:1 to 7:1, v/v) to afford compounds **12** (8 mg), **13** (3 mg) and **14** (2 mg). The *n*-butanol extract (2.3 g) was purified by RP-FC with MeOH–$H_2O$ (35:65 to 60:40, v/v) as mobile phase, followed by semi-preparative HPLC (MeOH–$H_2O$, 58:42, v/v) to yield compounds **15** (36 mg, $t_R$ 15.6 min) and **16** (45 mg, $t_R$ 16.5 min).

#### 2.3.1. Aloeresin K (**8**)

Yellowish amorphous powder; [$\alpha$]20 D = −130.2° (*c* 0.66, MeOH); UV (MeOH) $\lambda_{max}$: 226, 252 and 300 nm; IR (KBr) $\nu_{max}$: 3376 (br), 2934, 1706, 1650, 1600, 1379, 1246, 1164 and 1103 cm$^{-1}$; positive ESIMS *m/z* 599.19 [M + H]$^+$; HRESIMS *m/z* 621.1973 [M + Na]$^+$ (calcd. for $C_{31}H_{34}O_{12}Na$, 621.1942); $^1$H ($CD_3OD$, 400 MHz) and $^{13}$C NMR ($CD_3OD$, 100 MHz) spectral data see Table 1.

#### 2.3.2. 6′-O-acetyl-aloin B (**9**)

Yellow amorphous powder; [$\alpha$]20 D = −53.8° (*c* 0.66, MeOH); UV (MeOH) $\lambda_{max}$: 269, 297 and 356 nm; IR (KBr) $\nu_{max}$: 3403 (br), 2876, 1721, 1612, 1286, 1233 and 1069 cm$^{-1}$; positive ESIMS *m/z* 461.05 [M + H]$^+$; HRESIMS *m/z* 483.1279 [M + Na]$^+$ (calcd. for $C_{23}H_{24}O_{10}Na$, 483.1262); $^1$H ($CD_3OD$, 400 MHz) and $^{13}$C NMR ($CD_3OD$, 100 MHz) spectral data see Table 1.

#### 2.3.3. Aloeresin J (**10**)

Yellowish amorphous powder; [$\alpha$]20 D = −147.8° (*c* 0.69, MeOH); UV (MeOH) $\lambda_{max}$: 225, 251 and 297 nm; IR (KBr) $\nu_{max}$: 3385 (br), 2971, 2926, 1701, 1647, 1599, 1382, 1259, 1166 and 1078 cm$^{-1}$; positive ESIMS *m/z* 571.21 [M + H]$^+$; HRESIMS *m/z* 593.1998 [M + Na]$^+$ (calcd. for $C_{30}H_{34}O_{11}Na$, 593.1993); $^1$H ($CD_3OD$, 400 MHz) and $^{13}$C NMR ($CD_3OD$, 100 MHz) spectral data see Table 1.

#### 2.3.4. 6′-O-acetyl-aloin A (**11**)

Yellow amorphous powder; [$\alpha$]20 D = +5.2° (*c* 0.63, MeOH); UV (MeOH) $\lambda_{max}$: 269, 297 and 356 nm; IR (KBr) $\nu_{max}$: 3423 (br), 2920, 2872, 1728, 1622, 1236, 1101 and 1032 cm$^{-1}$; positive ESIMS *m/z* 461.08 [M + H]$^+$; HRESIMS *m/z* 483.1285 [M + Na]$^+$ (calcd. for $C_{23}H_{24}O_{10}Na$, 483.1262); $^1$H ($CD_3OD$, 400 MHz) and $^{13}$C NMR ($CD_3OD$, 100 MHz) spectral data see Table 1.

### 2.4. Expression and purification of PDE4D

The protocols for expression and purification of PDE4D were referred to our previous reports [19–22]. In brief, the recombinant plasmid pET15b subcloned with PDE4D2 (catalytic domain, residues 86–413) was introduced into the *E. coli* strains BL21 (codonplus) and the transformed cells were cultivated in LB medium containing 100 μg mL$^{-1}$ ampicillin and 0.4% glucose at 37 °C until $OD_{600}$ = 0.7. Then 0.1 mM isopropyl β-*D*-1-thiogalactopyranoside (IPTG) was applied to induce PDE4D protein expression for another 20 h at 15 °C. PDE4D protein was purified by Ni-NTA column eluted with imidazole buffer and the effluent was monitored through $OD_{280}$. Typically 40–60 mg of PDE4D was obtained from 1 L cell culture, with a purity of greater than 90% as determined by SDS-PAGE.

### 2.5. Enzymatic assays

The enzymatic activities of the catalytic domain of PDE4D were assayed by using $^3$H-cAMP as substrate. First, $^3$H-cAMP was diluted with the assay buffer containing 50 mM Tris–HCl

**Table 1**
$^{1}H$ (400 MHz) and $^{13}C$ (100 MHz) NMR data of compounds **8**, **9**, **10** and **11** in $CD_3OD$ ($\delta$ in ppm, $J$ in Hz).

| Carbon | 8 | | 10 | | 9 | | 11 | |
|---|---|---|---|---|---|---|---|---|
| | $\delta_C$ | $\delta_H$ mult. | $\delta_C$ | $\delta_H$ mult. | $\delta_C$ | $\delta_H$ mult. | $\delta_C$ | $\delta_H$ mult. |
| 1 | | | | | 162.9 | | 163.2 | |
| 2 | 167.2 | | 167.4 | | 114.1 | 6.85, s | 114.5 | 6.87, s |
| 3 | 112.6 | 6.12 (s) | 112.6 | 6.12 (s) | 152.3 | | 151.1 | |
| 4 | 182.2 | | 182.2 | | 117.2 | 6.96, s | 119.2 | 6.97, s |
| 5 | 144.8 | | 144.6 | | 121.3 | 6.98 (d, 7.4) | 119.4 | 6.90 (d, 7.4) |
| 6 | 112.6 | 6.77 (s) | 112.5 | 6.79 (s) | 136.0 | 7.44 (t, 7.9) | 137.0 | 7.45 (t, 7.9) |
| 7 | 162.0 | | 162.0 | | 117.4 | 6.84 (d, 8.1) | 116.6 | 6.81 (d, 8.1) |
| 8 | 111.4 | | 111.8 | | 163.0 | | 162.6 | |
| 9 | 44.9 | 2.83 (dd, 14.2, 5.0) | 44.6 | 2.90 (dd, 14.3, 4.5) | 195.4 | | 195.3 | |
| | | 2.76 (d, 7.8) | | 2.76 (d, 8.3) | | | | |
| 10 | 66.3 | 4.45 (m) | 66.0 | 4.48 (m) | 45.4 | 4.47 (d, 1.6) | 45.4 | 4.42 (d, 1.7) |
| 11 | 23.7 | 1.37 (d, 6.2) | 23.6 | 1.35 (d, 6.3) | 64.5 | 4.65 (s) | 64.6 | 4.66 (d, 3.1) |
| 5-$CH_3$ | 23.7 | 2.71 (s) | 23.6 | 2.72 (s) | | | | |
| 7-$OCH_3$ | 57.1 | 3.87 (s) | 57.0 | 3.88 (s) | | | | |
| 1a | 159.6 | | 159.6 | | 117.8 | | 117.9 | |
| 4a | 117.2 | | 117.2 | | 147.2 | | 142.3 | |
| 5a | | | | | 142.3 | | 146.9 | |
| 8a | | | | | 119.1 | | 118.8 | |
| 1′ | 72.8 | 5.20 (d, 10.1) | 72.8 | 5.19 (d, 10.1) | 85.9 | 3.28 (dd, 9.1, 2.5) | 85.9 | 3.28 (dd, 9.6, 1.8) |
| 2′ | 73.7 | 5.75 (dd, 9.8, 9.4) | 73.9 | 5.74 (dd, 9.9, 9.5) | 71.7 | 2.81 (t, 9.3) | 71.7 | 2.81 (t, 9.3) |
| 3′ | 77.7 | 3.75 (d, 9.0) | 77.9 | 3.75 (d, 8.8) | 79.7 | 3.25 (d, 9.1) | 79.7 | 3.25 (d, 9.6) |
| 4′ | 72.4 | 3.57 (m) | 72.3 | 3.57 (t, 8.9) | 71.5 | 3.07 (t, 9.3) | 71.4 | 3.06 (t, 9.3) |
| 5′ | 80.1 | 3.69 (m) | 82.9 | 3.47 (m) | 78.7 | 2.98 (m) | 78.8 | 2.98 (m) |
| 6′ | 64.4 | 4.46 (dd, 11.9, 1.5) | 63.1 | 3.94 (dd, 12.0, 1.9) | 64.7 | 4.06 (dd, 11.7, 2.0) | 64.5 | 4.07 (dd, 11.7, 2.0) |
| | | 4.26 (dd, 12.1, 6.4) | | 3.74 (dd, 11.9, 6.4) | | 3.77 (dd, 11.7, 7.1) | | 3.76 (dd, 11.7, 7.0) |
| $\underline{C}OCH_3$ | 173.0 | | | | 172.6 | | 172.6 | |
| $C\underline{O}CH_3$ | 20.9 | 2.03 (s) | | | 20.5 | 1.88 (s) | 20.5 | 1.88 (s) |
| 1″ | 168.0 | | 167.8 | | | | | |
| 2″ | 114.6 | 6.03 (d, 15.9) | 115.6 | 6.10 (d, 15.8) | | | | |
| 3″ | 146.6 | 7.35 (d, 16.1) | 146.1 | 7.39 (d, 15.8) | | | | |
| 4″ | 127.0 | | 128.2 | | | | | |
| 5″ | 131.1 | 7.31 (d, 8.6) | 130.9 | 7.42 (d, 8.7) | | | | |
| 6″ | 116.9 | 6.74 (d, 8.6) | 115.4 | 6.89 (d, 8.8) | | | | |
| 7″ | 161.3 | | 163.2 | | | | | |
| 8″ | 116.9 | 6.74 (d, 8.6) | 115.4 | 6.89 (d, 8.8) | | | | |
| 9″ | 131.1 | 7.31 (d, 8.6) | 130.9 | 7.42 (d, 8.7) | | | | |
| 7″-$OCH_3$ | | | 55.9 | 3.79 (s) | | | | |

(pH 7.5), 10 mM $MgCl_2$ and 0.5 mM DTT to $2 \times 10^4$–$3 \times 10^4$ cpm per assay. The reaction was carried out in a reaction mixture containing PDE4D enzyme, substrate and different concentrations of inhibitor dissolved in DMSO at room temperature for 15 min, and terminated by adding 0.2 M of $ZnSO_4$. Then the reaction product $^3$H-AMP was precipitated out by 0.2 N of $Ba(OH)_2$, whereas unreacted $^3$H-cAMP remained in the supernatant. The radioactivity in the supernatant was measured in 2.5 mL of Ultima Gold liquid scintillation cocktails by a liquid scintillation counter. All of isolates were preliminary screened at a concentration of 10 μM and the $IC_{50}$ values of active compounds were further measured by nonlinear regression. Each test was measured in triplicate. Rolipram, a representative PDE4 inhibitor, was selected as positive control.

### 2.6. Cytotoxic assays

The cytotoxicity of compounds **13** and **14** on the murine macrophage RAW 264.7 cells (obtained from ATCC, Manassas, VA, USA) was evaluated by MTT assay. RAW 264.7 cells were cultured in DMEM (Gibco-BRL, Grand Island, NY, USA) supplemented with 10% fetal bovine serum (Zhejiang Tianhang Biological Technology Co., Ltd., Hangzhou, China) in 5% $CO_2$ at 37 °C. Cells were seeded into 96-well culture plate with a density of $1 \times 10^4$ cells per well and allowed to adhere for 24 h, and then treated with various concentrations of each compound for another 24 h. After treatment, cells were incubated with 0.5 mg $mL^{-1}$ MTT solution for 4 h at 37 °C and then the supernatant was discarded and the formazan crystal was dissolved in DMSO. The optical density at 570 nm was measured on a FlexStation 3 microplate reader (Molecular Devices, Sunnyvale, CA, USA) with SoftMax Pro 5 software onboard.

## 3. Results and discussion

### 3.1. Structural elucidation of the isolated compounds

Compound **8** was obtained as a yellowish amorphous powder. Its molecular formula was established as $C_{31}H_{34}O_{12}$ from a pseudomolecular ion peak at $m/z$ 621.1973 $[M + Na]^+$ (calcd. for $C_{31}H_{34}O_{12}Na$, 621.1942) in the HRESIMS. The IR spectrum of **8** indicated the presence of hydroxyl group (3376 $cm^{-1}$, br), conjugated ester carbonyl (1706 $cm^{-1}$), chelated carbonyl group (1650 $cm^{-1}$) and aromatic moiety (1600 $cm^{-1}$). The UV spectrum gave maximum absorptions at 226, 252 and 300 nm, which were the characteristics of chromones [23]. The $^1$H-NMR spectroscopic data of **8** (Table 1) combined with its $^1$H–$^1$H COSY and HSQC spectra

exhibited an AA′BB′ system for two pairs of *ortho*-coupled aromatic proton signals at δ 7.31 (2H, d, $J = 8.6$ Hz) and δ 6.74 (2H, d, $J = 8.6$ Hz), a *trans*-olefinic bond proton signals at δ 7.35 (1H, d, $J = 16.1$ Hz) and δ 6.03 (1H, d, $J = 15.9$ Hz), two isolated aromatic proton signals on chromone skeleton at δ 6.77 (1H, s) and δ 6.12 (1H, s), a β-linked glucosyl moiety at δ 3.57–5.75 (anomeric proton at δ 5.20 (1H, d, $J = 10.1$ Hz)), a 2-hydroxypropyl group at δ 2.83 (1H, dd, $J = 14.2$, 5.0 Hz), δ 2.76 (1H, d, $J = 7.8$ Hz), δ 4.45 (1H, m) and δ 1.37 (3H, d, $J = 6.2$ Hz), a methoxyl group at δ 3.87 (3H, s), as well as two methyl groups at δ 2.71 (3H, s) and 2.03 (3H, s). The $^{13}$C-NMR spectrum, in combination with HSQC experiments and aforesaid analysis, indicated 31 carbons attributable to three carbonyl groups ($\delta_C$ 182.2, 173.0 and 168.0), eight $sp^2$ quaternary carbons ($\delta_C$ 167.2 (bearing oxygen atoms), 162.0, 161.3, 159.6, 144.8, 127.0, 117.2 and 111.4), eight $sp^2$ methines (146.6, 131.1, 116.9, 114.6 and 112.6), six glucosyl carbons ($\delta_C$ 80.1, 77.7, 73.7, 72.8, 72.4 and 64.4), a methoxy group ($\delta_C$ 57.1), a $sp^3$ methylene ($\delta_C$ 44.9), a $sp^3$ methine ($\delta_C$ 66.3), and three methyl groups ($\delta_C$ 23.7 and 20.9). The aforementioned data preliminary indicated that compound **8** was a 2,5,7,8-tetrasubstituted chromone. The chromone skeleton was confirmed by the key HMBC correlations (Fig. 2) of H-6 to C-4a and C-8, and H-3 to C-2 and C-4a. The 2-hydroxypropyl group, methoxyl group and methyl group were respectively attached to C-2, C-7 and C-5 of the chromone ring, as indicated by the HMBC correlations of H-9 to C-2, the protons of methoxy to C-7, and the protons of methyl to C-4a, C-5 and C-6, respectively. β-glucosyl moiety was detected as being connected to C-8 due to the HMBC correlations of H-1′ to C-8 and C-1a. The HMBC correlations from H-5″ to C-3″, H-2″ to C-1″ and H-3″ to C-1″ implied the presence of a *p*-(*E*)-coumaroyl. The above-mentioned information was quite similar to that of isoaloeresin D (**1**), except for the presence of an additional acetyl group ($\delta_H$ 2.03, 3H, s; $\delta_C$ 20.9 and 173.0). The location of the acetyl group was assigned at 6′-OH by an HMBC correlation from H-6′ to the carbonyl group at $\delta_C$ 173.0. The absolute configuration of the hydroxy-bearing carbon (C-10) of the 2-hydroxypropyl chain in **8** was assigned by acid-catalyzed hydrolysis method. Approximate 1 mg of compound **8** was refluxed with 1 mL of 1 M HCl (MeOH–$H_2O$, 3:1, v/v) for 1 h to convert **8** to **8a**. After removal of solvent and HCl under vacuum, the residue was dissolved in MeOH and analyzed by HPLC using the previously reported procedures [24]. The *S* absolute configuration of C-10 was confirmed by comparison of the retention time of **8a** ($t_R$ 11.3 min) with reference standard. Thus, compound **8** was identified as 6′-*O*-acetyl-isoaloeresin D, and was given the trivial name aloeresin K.

Compound **9**, a yellow amorphous powder, possessed a molecular formula of $C_{23}H_{24}O_{10}$, as established by HRESIMS (*m/z* 483.1279 $[M + Na]^+$, calcd. for $C_{23}H_{24}O_{10}Na$, 483.1262). The IR spectrum of **9** showed absorption bands for hydroxyl

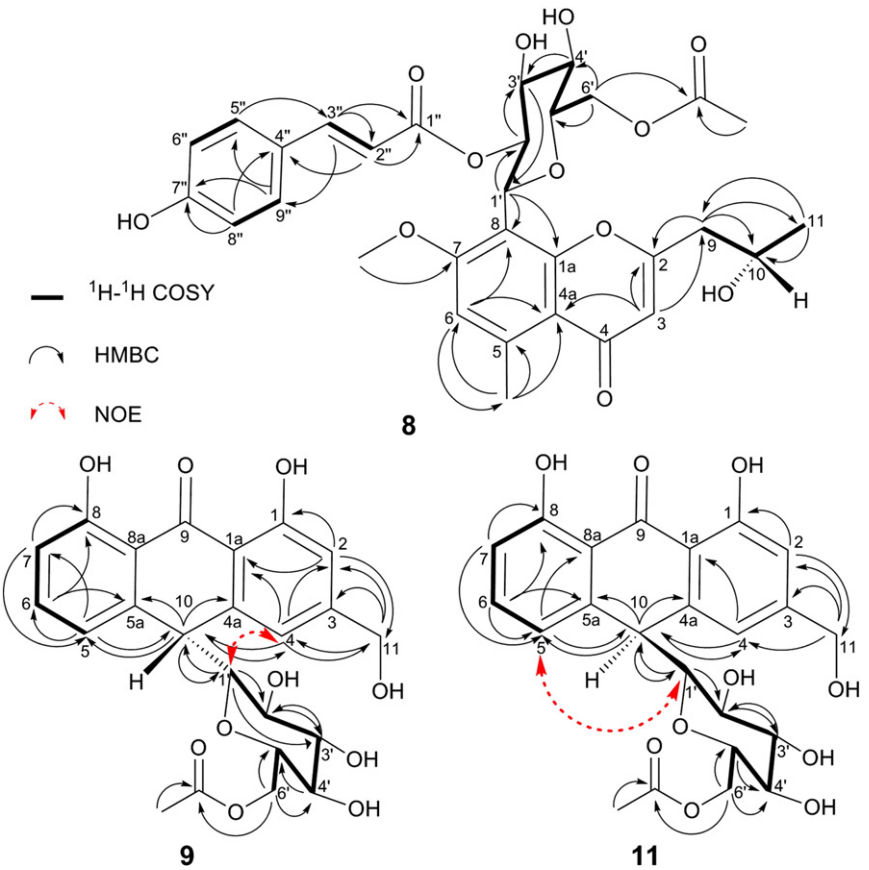


**Fig. 2.** Selected $^1$H–$^1$H COSY, HMBC and NOE correlations of compounds **8**, **9** and **11**.

group (3403 $cm^{-1}$, br), ester carbonyl (1721 $cm^{-1}$) and chelated carbonyl group (1612 $cm^{-1}$). The UV absorption bands at $\lambda_{max}$ 269, 297 and 356 nm implied the presence of an anthrone chromophore [25]. The $^1$H-NMR (Table 1) and HSQC spectra of **9** exhibited signals for three vicinal aromatic protons at δ 6.98 (1H, d, $J$ = 7.4 Hz), δ 7.44 (1H, t, $J$ = 7.9 Hz) and δ 6.84 (1H, d, $J$ = 8.1 Hz), as well as two isolated aromatic protons at δ 6.96 (1H, s) and δ 6.85 (1H, s) belonging to the anthrone ring. Combined with the signals of two strongly chelated phenol protons at δ 11.88 (1H, s) and δ 11.87 (1H, s) and typical H-10 signals at δ 4.47 (1H, d, $J$ = 1.6 Hz), compound **9** was deduced as a 1,8-dihydroxyl-3,10-disubstituted anthrone. The spectra also showed a β-linked glucosyl group at δ 2.81–4.06 (anomeric proton at δ 3.28 (1H, dd, $J$ = 9.1, 2.5 Hz)), a hydroxymethyl at δ 4.65 (2H, s), and a methyl group at δ 1.88 (3H, s). The $^{13}$C-NMR spectrum together with the HSQC experiment revealed 23 carbon signals including those of two carbonyl groups ($\delta_C$ 195.4 and 172.6), seven $sp^2$ quaternary carbons ($\delta_C$ 163.0, 162.9, 152.3, 147.2, 142.3, 119.1 and 117.8, two of them bearing oxygen atoms), five $sp^2$ methines ($\delta_C$ 136.0, 121.3, 117.4, 117.2 and 114.1), six glucosyl carbons ($\delta_C$ 85.9, 79.7, 78.7, 71.7, 71.5 and 64.7), an oxygenated methylene ($\delta_C$ 64.5), a $sp^3$ methine ($\delta_C$ 64.5), together with two methyl groups ($\delta_C$ 45.4 and 20.5). The HMBC correlations (Fig. 2) from hydroxymethyl protons ($\delta_H$ 4.65, H-11) to C-2, C-3 and C-4 indicated that a hydroxymethyl was attached to C-3 of the anthrone ring. The location of glucosyl moiety was assigned at C-10 by an HMBC correlation from the anomeric proton ($\delta_H$ 3.28, H-1′) to C-10. An acetyl group was located at 6′-OH as indicated by the HMBC correlations of H-6′ to the carbonyl group at $\delta_C$ 172.6. The NOESY interactions of H-4 and H-1′ (Fig. 2) further assigned the *R* configuration of C-10 [26]. Hence, compound **9** was assigned as an aloin-like compound named 6′-*O*-acetyl-aloin B.

Compound **11**, a yellow amorphous powder, possessed the same molecular formula as that of **9**, implying that they were isomers. The $^1$H and $^{13}$C NMR spectra of **11** and **9** (Table 1) were almost identical. The NOESY associations of H-5 with H-1′ (Fig. 2) suggested the *S* configuration of C-10 in **11**. Their absolute configuration was confirmed by comparison of corresponding optical rotation ([α]20 D + 5.2° and − 53.8° for **11** and **9**, respectively) with aloin-like isomers as well [27]. Therefore, compound **11**, the diastereoisomer of **9**, was elucidated as 6′-*O*-acetyl-aloin A.

Compound **10** had previously been identified from *Aloe rubroviolacea* Schweinf. by LC-MS method [28]. The present study gave a detailed description of its NMR data (Table 1) and absolute configuration for the first time. The methoxyl group was confirmed being connected to C-7″ by HMBC correlations of methoxyl protons ($\delta_H$ 3.79) to C-7″ ($\delta_C$ 163.2). Using the same procedure as compound **8**, **10** was converted to **8a** by acid-catalyzed hydrolysis. Hence, the absolute configuration of C-10 in **10** was assigned as *S*. Compound **10** was given the trivial name aloeresin J.

The other twelve known compounds were identified as isoaloeresin D (**1**) [29], aloin B (**2**) [26], aloin A (**3**) [26], aloin-dimer A (**4**) [30], aloin-dimer B (**5**) [30], aloin-dimer C (**6**) [30], aloin-dimer D (**7**) [30], aloe-emodin (**12**) [31], elgonica-dimer A (**13**) [32], elgonica-dimer B (**14**) [32], aloinoside B (**15**) [33] and aloinoside A (**16**) [33] by comparison of their spectroscopic data with those reported in literatures.

### 3.2. In vitro inhibitory activity towards PDE4D

All of the isolates were screened for their inhibitory activity against PED4D. The positive control, rolipram, herein gave an $IC_{50}$ value of 0.59 μM, which was comparable to the literature data of 1.0 μM. The bioassay results indicated that compounds **13** and **14** exhibited remarkable inhibitory activity towards PDE4D (Table 2), with $IC_{50}$ values of 9.25 and 4.42 μM, respectively. The inhibitory curves of compounds **13**, **14** and rolipram were represented in Fig. 3.

Interestingly, it was found that anthraquinones with 10-carbonyl group like compounds **12**, **13** and **14** showed remarkable enzyme inhibitory activity, while anthrones including compounds **2**–**7**, **9**, **11**, **15** and **16** were inactive. These results verified our previous structure–activity relationship (SAR) observation that anthraquinones with glucosyl group on C-10 of the ring decreased inhibitory activity against PDE4D [18]. Compounds **13** and **14** are a pair of diastereoisomers differing in the configuration of C-10. They are anthrone–anthraquinone dimers composed of anthrone emodin-10′-*C*-β-D-glucopyranoside and anthraquinone aloe-emodin moieties [34]. Our previous study showed that their subunit aloe-emodin (**12**) exhibited moderate inhibitory activity with an $IC_{50}$ of ≈20 μM [18]. Taken together, it can be concluded that anthraquinone ring may contribute to good activity. However, further investigation should be carried out to explore their inhibitory mechanism.

For further study, RAW 264.7 cell, which is the most common used cell line in *in vitro* anti-inflammatory experiment, was applied to the cytotoxicity test of active compounds. MTT assays (Table 2) indicated that compounds **13** and **14** did not show significant cytotoxicity when the concentration was up to 50 μM.

In summary, two new anthrones (**9** and **11**) and one new chromone (**8**), as well as thirteen known compounds, were isolated from the 95% EtOH extract of *A. barbadensis* leaf skin. In the bioassay of PDE4D, compounds **13** and **14** were found to be PDE4D inhibitors, with their $IC_{50}$ values of 9.25 and 4.42 μM, respectively. These achievements can provide evidences for the use of *A. barbadensis* leaf skin as functional feed additives for anti-inflammatory purpose.

## Conflict of interest

The authors declare no conflict of interest.

## Acknowledgments

This work is financially supported by the National Key Technology R&D Program during the Twelfth Five-Year Plan Period of People's Republic of China (No. 2013BAD10B04-2),

**Table 2**
$IC_{50}$ values of compounds **13** and **14** against PDE4D and their cytotoxicity.

| Compound | $IC_{50}$ (μM) | Cell viability (%)[a] |
|---|---|---|
| **13** | 9.25 ± 0.64 | 98.3 ± 2.8 |
| **14** | 4.42 ± 0.74 | 100.5 ± 2.4 |
| Rolipram[b] | 0.59 ± 0.05 | |

[a] Determined on RAW 264.7 cell line at 50 μM.
[b] Positive control.

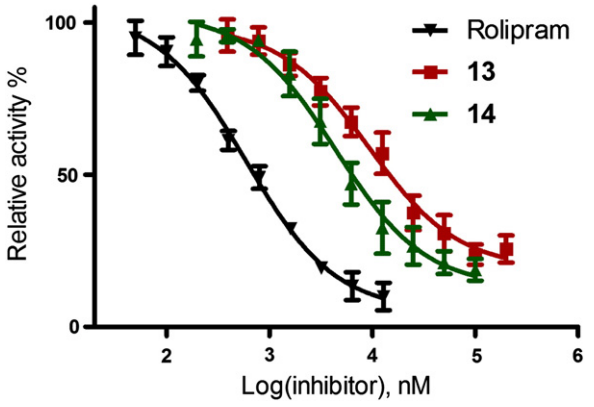


**Fig. 3.** Inhibitory curves of compounds **13**, **14**, and rolipram (positive control) against PDE4D.

the Guangzhou Science and Technology Programs (Nos. 2014J4100176 & 2014J4100165), the National Natural Science Foundation of China (No. 81373258), and Guangdong Natural Science Foundation (No. S2013010014867).

## Appendix A. Supplementary data

Supplementary data to this article can be found online at http://dx.doi.org/10.1016/j.fitote.2014.11.018.

## References

[1] Chow JTN, Williamson DA, Yates KM, Goux WJ. Chemical characterization of the immunomodulating polysaccharide of *Aloe vera* L. Carbohydr Res 2005;340:1131–42.
[2] Waller GR, Mangiafico S, Ritchey CR. A chemical investigation of *Aloe barbadensis* Miller. Proc Okla Acad Sci 1978;58:69–76.
[3] Chinchilla N, Carrera C, Duran AG, Macias M, Torres A, Macias FA. *Aloe barbadensis*: how a miraculous plant becomes reality. Phytochem Rev 2013;12:581–602.
[4] Ni Y, Turner D, Yates KM, Tizard I. Isolation and characterization of structural components of *Aloe vera* L. leaf pulp. Int Immunopharmacol 2004;4:1745–55.
[5] Reynolds T. The compounds in *Aloe* leaf exudates: a review. Bot J Linn Soc 1985;90:157–77.
[6] Bozzi A, Perrin C, Austin S, Vera FA. Quality and authenticity of commercial aloe vera gel powders. Food Chem 2007;103:22–30.
[7] Lee KY, Weintraub ST, Yu BP. Isolation and identification of a phenolic antioxidant from *Aloe barbadensis*. Free Radic Biol Med 2000;28:261–5.
[8] Pecere T, Gazzola MV, Mucignat C, Parolin C, Vecchia FD, Cavaggioni A, et al. Aloe-emodin is a new type of anticancer agent with selective activity against neuroectodermal tumors. Cancer Res 2000;60:2800–4.
[9] Dai JB, Luo BJ, Su WM. Comprehensive utilization aloe skin processing method, Patent CN 101258922 B, 2012.
[10] Liu SP, Mansour MN, Dillman KS, Perez JR, Danley DE, Aeed PA, et al. Structural basis for the catalytic mechanism of human phosphodiesterase 9. Proc Natl Acad Sci U S A 2008;105:13309–14.
[11] Bender AT, Beavo JA. Cyclic nucleotide phosphodiesterases: molecular regulation to clinical use. Pharmacol Rev 2006;58:488–520.
[12] Menniti FS, Faraci WS, Schmidt CJ. Phosphodiesterases in the CNS: targets for drug development. Nat Rev Drug Discov 2006;5:660–70.
[13] Burgin AB, Magnusson OT, Singh J, Witte P, Staker BL, Bjornsson JM, et al. Design of phosphodiesterase 4D (PDE4D) allosteric modulators for enhancing cognition with improved safety. Nat Biotechnol 2010;28:63–70.
[14] Lipworth BJ. Phosphodiesterase-4 inhibitors for asthma and chronic obstructive pulmonary disease. Lancet 2005;365:167–75.
[15] Wang C, Yang XM, Zhuo YY, Zhou H, Lin HB, Cheng YF, et al. The phosphodiesterase-4 inhibitor rolipram reverses Aβ-induced cognitive impairment and neuroinflammatory and apoptotic responses in rats. Int J Neuropsychopharmacol 2012;15:749–66.
[16] Park SJ, Ahmad F, Philp A, Baar K, Williams T, Luo HB, et al. Resveratrol ameliorates aging-related metabolic phenotypes by inhibiting cAMP phosphodiesterases. Cell 2012;148:421–33.
[17] Gretarsdottir S, Thorleifsson G, Reynisdottir ST, Manolescu A, Jonsdottir S, Jonsdottir T, et al. The gene encoding phosphodiesterase 4D confers risk of ischemic stroke. Nat Genet 2003;35:131–8.
[18] Zhong JS, Huang YY, Ding WJ, Wu XF, Wan JZ, Luo HB. Chemical constituents of *Aloe barbadensis* Miller and their inhibitory effects on phosphodiesterase-4D. Fitoterapia 2013;91:159–65.
[19] Li Z, Cai YH, Cheng YK, Lu X, Shao YX, Li X, et al. Identification of novel phosphodiesterase-4D inhibitors prescreened by molecular dynamics-augmented modeling and validated by bioassay. J Chem Inf Model 2013;53:972–81.
[20] Chen SK, Zhao P, Shao YX, Li Z, Zhang CX, Liu PQ, et al. Moracin M from *Morus alba* L. is a natural phosphodiesterase-4 inhibitor. Bioorg Med Chem Lett 2012;22:3261–4.
[21] Liu YN, Huang YY, Bao JM, Cai YH, Guo YQ, Liu SN, et al. Natural phosphodiesterase-4 (PDE4) inhibitors from *Crotalaria ferruginea*. Fitoterapia 2014;94:177–82.
[22] Cheng ZB, Deng YL, Fan CQ, Han QH, Lin SL, Tang GH, et al. Prostaglandin derivatives: nonaromatic phosphodiesterase-4 inhibitors from the soft coral *Sarcophyton ehrenbergi*. J Nat Prod 2014;77:1928–36.
[23] Ganguly BK, Bagchi P. Studies on the ultraviolet absorption spectra of coumarins and chromones. Part I. J Org Chem 1956;21:1415–9.
[24] Zhong JS, Wan JZ, Liu YP, Ding WJ, Wu XF, Xie ZY. Simultaneous HPLC quantification of seven chromones in *Aloe barbadensis* Miller using a single reference standard. Anal Methods 2014;6:4388–95.
[25] Yenesew A, Dagne E, Müller M, Steglich W. An anthrone, an anthraquinone and two oxanthrones from *Kniphofia foliosa*. Phytochemistry 1994;37:525–8.
[26] Manitto P, Monti D, Speranza G. Studies on aloe. Part 6. Conformation and absolute configuration of aloins A and B and related 10-*C*-glucosyl-9-anthrones. J Chem Soc Perkin Trans 1990;1:1297–300.
[27] Okamura N, Hine N, Harada S, Fujioka T, Mihashi K, Nishi M, et al. Diastereomeric *C*-glucosylanthrones of *Aloe vera* leaves. Phytochemistry 1997;45:1519–22.
[28] Schmidt J, Blitzke T, Masaoud M. Structural investigations of 5-methylchromone glycosides from *Aloe* species by liquid chromatography/electrospray tandem mass spectrometry. Eur J Mass Spectrom 2001;7:481–90.
[29] Okamura N, Hine N, Harada S, Fujioka T, Mihashi K, Yagi A. Three chromone components from *Aloe vera* leaves. Phytochemistry 1996;43:495–8.
[30] Shindo T, Ushiyama H, Kan K, Uehara S, Yasuda K, Takano I, et al. Structural analyses of barbaloin-related compounds in aloe drinks. J Food Hyg Soc Jpn 2002;43:115–21.
[31] Sanchez JF, Entwistle R, Hung JH, Yaegashi J, Jain S, Chiang YM, et al. Genome-based deletion analysis reveals the prenyl xanthone biosynthesis pathway in *Aspergillus nidulans*. J Am Chem Soc 2011;133:4010–7.
[32] Shin KH, Woo WS, Lim SS, Shim CS, Chung HS, Kennelly EJ, et al. Elgonica-dimers A and B, two potent alcohol metabolism inhibitory constituents of *Aloe arborescens*. J Nat Prod 1997;60:1180–2.
[33] Gao J, Zhang GG, Dai RH, Bi KS. Isolation of aloinoside B and metabolism by rat intestinal bacteria. Pharm Biol 2005;42:581–7.
[34] Conner JM, Gray AI, Waterman PG, Reynolds T. Novel anthrone–anthraquinone dimers from *Aloe elgonica*. J Nat Prod 1990;53:1362–4.